Hierarchically Mesoporous–Macroporous Bioactive Glasses Scaffolds for Bone Tissue Regeneration

Hui-suk Yun,[1] Seung-eon Kim,[1] Yong-taek Hyun,[1] Su-jin Heo,[1,2] Jung-wook Shin[2]

[1] Center for Future Technology, Korea Institute of Materials Science, Changwon, Gyeongnam, South Korea 641-83

[2] Department of Bio-medical Engineering, Inje University, Gimhae, Gyeongnam, South Korea 621-749

Received 22 October 2007; revised 2 March 2008; accepted 17 March 2008
Published online 24 April 2008 in Wiley InterScience (www.interscience.wiley.com). DOI: 10.1002/jbm.b.31114

Abstract: Hierarchically 2D/3D mesoporous–macroporous bioactive glasses (MMBG) with good molding capabilities and compressive modulus were synthesized by sol–gel method and evaporation-induced self-assembly process in the presence of both nonionic triblock copolymers, $EO_{70}PO_{20}EO_{70}$ (P123) or $EO_{100}PO_{65}EO_{100}$ (F127), templates and methyl cellulose template. P123 or F127 acts as both a template, inducing the formation of mesopore, and an effective dispersant of MC, which produces macropores. *In vitro* bioactivity studies were carried out in simulated body fluid and showed superior bone-forming bioactivities of hierarchical MMBG. Human osteoblastlike cells, MG63, were seeded on MMBG and were determined using MTT [3-(4,5-dimethylthiazol-2-yl)-2,5,-diphenyl-tetrazolium bromide] assay to confirm biocompatibilities of MMBG. © 2008 Wiley Periodicals, Inc. J Biomed Mater Res Part B: Appl Biomater 87B: 374–380, 2008

Keywords: bioactive glass; bone tissue engineering; mesoporous–macroporous; polymer templating; self-assembly

INTRODUCTION

Mesoporous materials, which have pores ranging in size from 2 to 50 nm, have received enormous attention owing to their potential applications in catalysis, separation, sensing, and so on.[1] Their regular, tunable pore size, together with their large pore volume, should enable them to be used in a variety of host of biomedical and biotechnological applications, such as drug delivery and enzyme immobilization.[2–4] Recently, the use of these materials in bone tissue regeneration has also been proposed, because their large surface area and pore volume may enhance their bioactive behavior and allow them to be loaded with osteogenic agents to promote new bone formation.[3–13] Studies related to tissue regeneration accelerated after the development of mesoporous bioactive glasses (MBGs) by Zhao et al. in 2004.[7] Zhao et al. successfully synthesized hexagonally ordered MBGs by templating with a triblock copolymer, P123, and demonstrated their superior bone-forming bioactivities *in vitro* compared to normal BGs.[7–9] MBGs with a three-dimensional (3D) cubic pore structure were also successfully synthesized by our group using a template with the triblock copolymer, F127.[10] Stucky and coworkers reported the synthesis of MBG cement that exhibited the desired plasticity and rapid-setting capability, as well as a spherical MBG with hemostatic activity.[12,13] Although all of the reported MBGs show superior bone-forming activities, they are difficult to use as scaffolds for the regeneration of bone tissues at this stage, because their mesosized pores are too small to promote cell seeding, migration, and tissue in-growth. Suitable tissue scaffolds should have features such as a high porosity along with a macropore size in the range of 10–1000 μm and 3D interconnected pore structures, in order for them to have the permeability and diffusion properties required to promote the in-growth of bone cells.[14–16] BGs with hierarchical porosity, having interconnected pores in the meso and macrosize ranges, might exhibit the combined advantages of high surface areas from the mesopores and increased mass transport associated with the macropores.[14,17–19]

We report here the process, which can be used for the efficient and reproducible preparation of hierarchically MMBGs using a combination of the sol–gel, evaporation-induced self-assembly (EISA), and multipolymer templating processes. The triblock copolymer, P123 or F127, acts as both a template, inducing the formation of mesopore, and an effective dispersant of the large block copolymer, methyl cellulose (MC), which produces macropores. The hierarchically porous BGs so obtained have good molding capabilities and superior *in vitro* bone-forming bioactivities as well as favorable biocompatibilities.

Correspondence to: H.-s. Yun (e-mail: yuni@kims.re.kr)

EXPERIMENTAL PROCEDURES

Preparation of MMBG

The MMBG with cubic mesostructure was prepared using tetraethyl orthosilicate (TEOS), triethyl phosphate (TEP), and calcium nitrate tetrahydrate (CaNT) as inorganic precursors, a triblock copolymer, Pluronic F127 (average M_n = 12,600) as the mesostructure-directing agent through an EISA, and MC (average M_n = 86,000, viscosity = 4000 cps) as both the macrostructure-directing agent and binder. In a typical synthesis, 2.88 g of F127 is dissolved in 18.1 mL of ethanol (EtOH). Stock solutions, which were prepared by mixing 1.36 g of CaNT, 0.26 mL of TEP, 6 mL of TEOS, 0.95 mL of HCl (1*M*), 7.62 mL of EtOH, and 2.86 mL of H_2O, were added to this solution after stirring them for 1 h separately and were vigorously stirred together for another 4 h at 40°C. 4 g of MC was then mixed with this sol solution and was ultrasonic-treated for 5 min to make the homogeneous sol paste. The sol paste was transferred to a Teflon vessel with a Teflon seal and aged at 40°C and 40% RH for 24 h. The obtained gel block were molded and calcined at 600°C for 6 h in air to remove both templates. The molar composition of the gel paste was TEOS:CaNT:TEP:F127:MC = 1:0.2:0.05:0.008:0.0016 in this case. The MMBG with hexagonal mesostructure was prepared using same method, but a triblock copolymer was changed from F127 to Pluronic P123 (average M_n = 5750). The NoTri-BG was prepared using same method of MMBG, but the triblock copolymer was not used. The NoCaP-MMBG-F127 was also synthesized using similar method of MMBG, but CaNT and TEP was not used.

Characterizations

Structural characterization was carried out using X-ray diffraction (XRD; θ–2θ scanning, Philips-X'pert MPD 3040), Cu Kα (λ = 1.5406 Å) radiation (40 kV–40 mA), transmission electron microscopy (TEM; JEOL-JEM2100F) with field emission gun at 200 kV, and field emission scanning electron microscopy (FE-SEM; Hitachi-S5500 and JEOL-5800) at an accelerating voltage of 1–5 kV. The specific surface area and porosity was measured by N_2 adsorption method (BelJapan-Belsorp mini II) and the mercury porosimeter (Quantachrome-PoreMaster). The compressive strengths and modulus were determined using a microload system (R&B) at 0.5 mm/min of head speed set. Concentrations of Ca as well as pH of solutions after soaking each porous BG at different periods were determined by inductive-coupled plasma (ICP) atomic emission spectroscopy and pH system (Mettler Toledo).

In Vitro Bioactivity Test

The assessment of the *in vitro* bioactivity of the each obtained porous BG was carried out in simulated body fluid (SBF) at 37°C. Before immersing porous BGs in SBF, they were treated using an alternate soaking process[20]: The porous BGs were soaked in 300 mL of calcium chloride ($CaCl_2$, 200 m*M*) for 10 s and then rinsed with excess water. The porous BGs were subsequently soaked in a solution of potassium hydrogen phosphate trihydrate ($K_2HPO_4{\cdot}3H_2O$, 200 m*M*) and then rinsed with excess water. These steps were repeated three times and MBGs rinsed well. The porous BGs were immersed in SBF after drying. The SBF contained 142.0 m*M* Na^+, 5 m*M* K^+, 1.5 m*M* Mg^{2+}, 2.5 m*M* Ca^{2+}, 147.8 m*M* Cl^-, 4.2 m*M* HCO^{3-}, 1.0 m*M* HPO_4^{2-}, and 0.5 m*M* SO_4^{2-}.[21] Its chemical composition was similar to that of human plasma. The solution had a pH of 7.4 and was kept at 37°C before use. After soaking, each porous BG was collected from SBF, rinsed with acetone, and air-dried at 40°C.

In Vitro Biocompatibility Test

Human osteoblastlike cells, MG63, were seeded onto square-shaped specimens (height = 8 mm, width = 8 mm, depth = 3 mm) at a density of 1×10^4 cells/mL and cultured with Dulbecco's modified Eagle medium, 10% fetal bovine serum (FBS), and 1% Penicillin/Streptomycin. The cell culture was maintained in a gas-jacket incubator equilibrated with 5% CO_2 gas at 37°C. Cell medium was changed everyday. The cell viability and proliferation were determined using the MTT assay. The absorbance of the formazan produced by the cells was measured at 570 nm with a microplate reader (ELISA). Five specimens were examined for each sample.

RESULTS AND DISCUSSION

Fabrication of MMBG

The synthesis strategy is illustrated in Scheme 1. We preliminarily prepared the mixed sol solution of inorganic species (Si-, Ca-, P-) and triblock copolymer, P123 or F127, to produce the hexagonal- or cubic-mesostructured BG precursor, respectively. MC was then mixed with this sol solution to use as the template for producing the macrostructure, as well as to act as a binder. MC is an alternate block copolymer with a highly substituted hydrophobic region and less substituted hydrophilic region.[22] MC prefers to form a micelle structure having a hydrophilic part associated with water and this micelle formation increases the viscosity and subsequently induces the gelation of the MC. The gel paste was transferred to a Teflon vessel and was evaporated at a certain temperature and humidity to accelerate self-assembly. The obtained gel block has sufficient plasticity to be cut and shaped, which is important for the repair of irregular shaped defects in bones, as shown in Figure 1(a,b). The molded gel blocks were well preserved after the removal of both polymer templates, with no deformation or cracks caused by their calcination at 600°C [Figure 1(c)], although

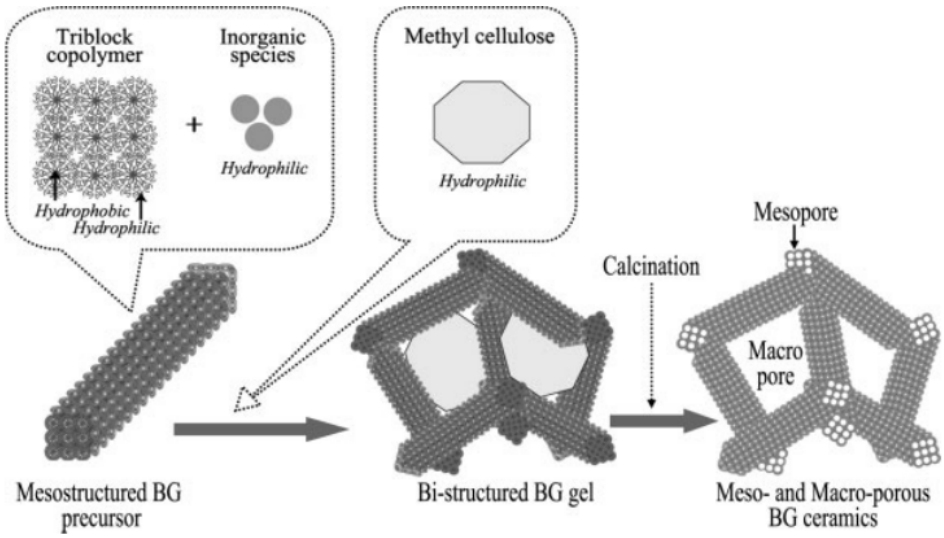

Scheme 1. Synthesis of hierarchically porous bioactive glasses.

it caused an ~25% decrease in their size, due to the condensation of the BG.

Characterization of MMBG

The calcined MMBG, which was synthesized using the P123 template (MMBG-P123), had a 2D hexagonal mesostructure, and this structure was well maintained after mixing it with MC, as revealed by the small angle X-ray diffraction (XRD) patterns [Figure 2(a)] and transmission electron microscopy (TEM) image [Figure 3(a)]. The 3D ordered cubic mesostructure of the MMBG produced by F127 template (MMBG-F127) was also successfully retained after mixing it with MC, as shown in Figures 2(b) and 3(b). It is worth noting that the presence of a triblock copolymer such as P123 and F127 is very effective in producing a uniform distribution of MC in the BG sol. According to the results, the macrosized pores (10–50 μm) were homogeneously produced in the MBG [Figure 3(d,e)], while only heterogeneously distributed giant-sized pores (>100 μm) were observed without the triblock copolymer [Figure 3(f)], as shown in the field emission scanning electron microscopy (FE-SEM) results. The features of the frame wall, which was composed of macrosized pores, apparently reflect the macroscopic particle morphology of their mesostructure. That is to say, in our synthetic method, the triblock copolymer and inorganic species (Si-, Ca-, P-) first produce mesostructured BG composites and then their hydrophilic region associates with the hydrophilic portion of the MC micelles (Scheme 1). Homogeneous interactions between the mesostructured BG particles and MC subsequently conduce homogeneously distributed and a well-interconnected 3D macropore structure with a relative porosity of 75–90%, as measured by mercury intrusion porosimetry. The 3D macropore structure has cancellous architecture, which is similar to cancellous bone structure.

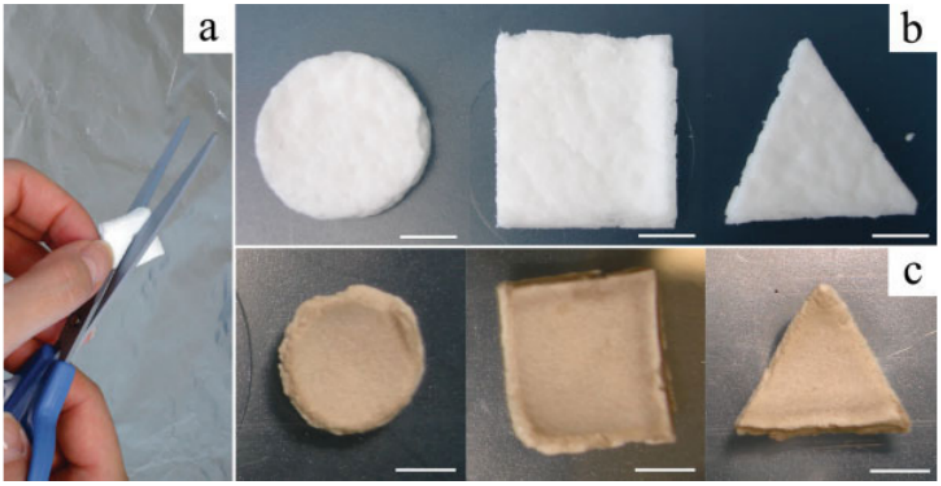

Figure 1. Digital images of MMBG: (a, b) as-synthesized and (c) calcined for 6 h at 600°C (bar = 10 mm). [Color figure can be viewed in the online issue, which is available at www.interscience.wiley.com.]

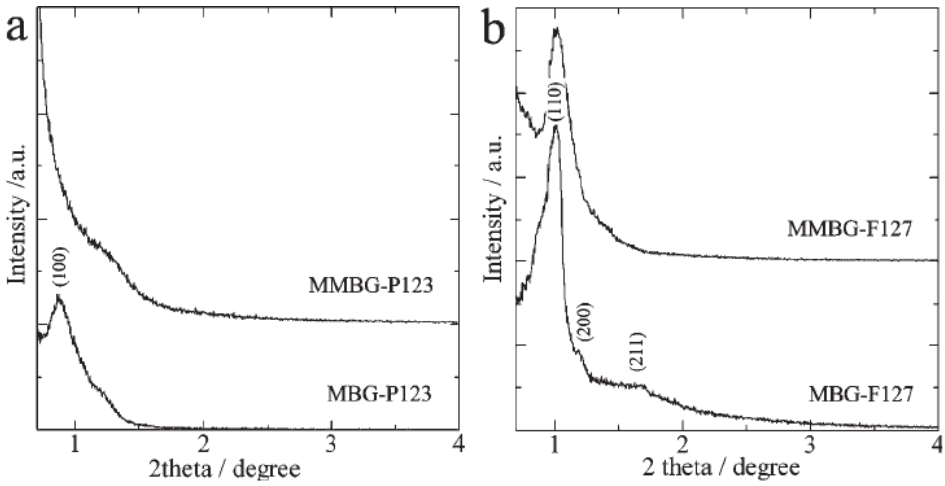

Figure 2. XRD patterns of (a) MMBG-P123 and (b) MMBG-F127. MBG-P123 and MBG-F127 are mesoporous BG without MC using by P123 and F127 templates, respectively.

On the other hand, the use of the NoTri-BG only leads to the formation of heterogeneously distributed giant pores with a relative porosity of 40–50%, due to the irregularly distributed aggregations of MC. The MMBG series had much higher compressive modulus than the BG, which was synthesized using the same method but without the triblock copolymer (designated NoTri-BG). The compressive moduli of the MMBG-F127 and MMBG-P123 specimens were measured to be 7.0 ± 0.3 and 20.9 ± 0.9 MPa, respectively, while that of NoTri-BG was measured to be 3.1 ± 1.9 MPa. The enhancement effect of the compressive modulus of the MMBG specimens is apparently related to their macropore structures. MMBG-P123 had a superior compressive modulus, because MBG-P123 bends for forming long fibrous macrostructure and MMBG-P123 consequently tends to form a cancellous structure.

Bioactivity of MMBG

BGs have been widely studied, because they have the ability to chemically bond with living bone tissue through the formation of a biologically active apatite layer at the implant–tissue interface.[23–26] The high porosity in the sol–gel BG favors the formation of an apatitelike layer, since it facilitates the rapid and massive release of Ca^{2+} ions leading to their saturation and affecting the pH in the medium, and induces the formation of silanol groups on the glass surface, leading to the nucleation and crystallization of apa-

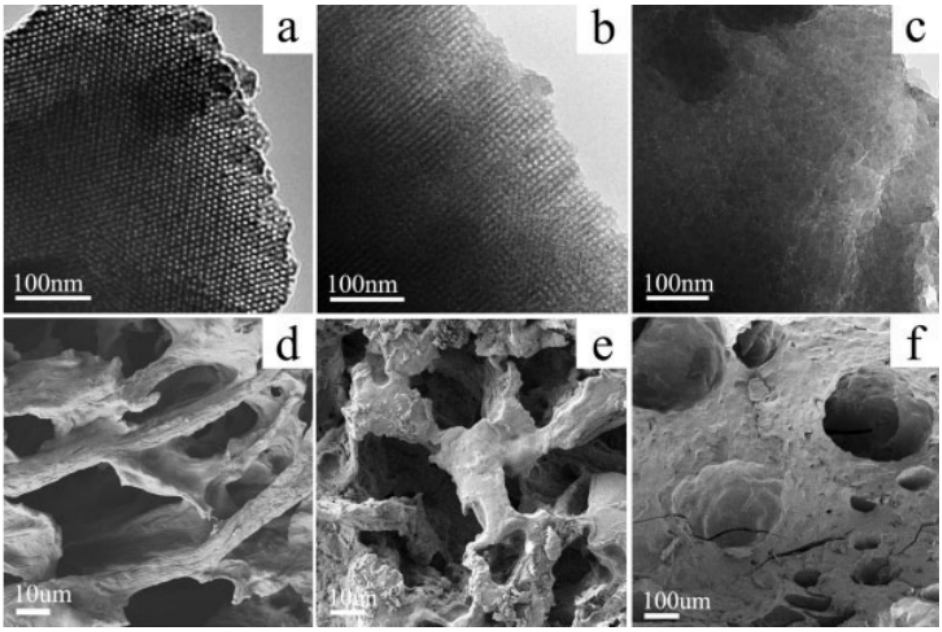

Figure 3. TEM images of (a) MMBG-P123, (b) MMBG-F127, and (c) NoTri-BG. (d), (e), and (f) are the FE-SEM micrographs of (a), (b), and (c), respectively. The samples were calcined for 6 h at 600°C.

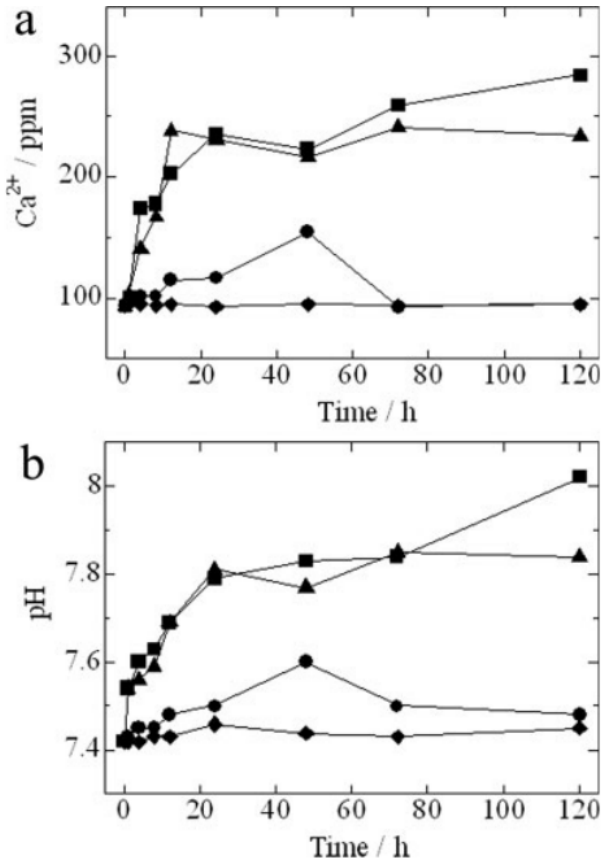

Figure 4. Variations of (a) calcium content and (b) pH values of the SBF as a function of soaking time for the MMBG-F127 (■), MMBG-P123 (▲), NoTri-BG (●), and NoCaP-MMBG-F127 (◆). NoCaP-MMBG-F127 is a mesoporous silica without Ca and P.

tite. Figure 4 shows the Ca^{2+} concentrations and pH values of SBF for different soaking times of MMBG-F127, MMBG-P123, NoTri-BG, and NoCaP-MMBG-F127. The Ca^{2+} levels rapidly increase for MMBG-F127 during the first 12 h of soaking [Figure 4(a)]. Thereafter, the Ca^{2+} concentration in SBF slowly decreases until 48 h and then slowly increases again until the end of the assay. The pH evolution follows a profile analogous to that of the Ca^{2+} content [Figure 4(b)]. The pH level sharply increases during the very first hour of the test for MMBG-F127 and then gradually increases during the next 24 h. The pH level then decreases once and increases again until the end of the assay. These results indicate that a rapid Ca^{2+}-H^{+} exchange occurs between the MMBG and the SBF. The fast ion exchange between MMBG and SBF allows for the rapid deposition of apatite on MMBG. Similar phenomena concerning the change of the Ca^{2+} concentration and pH value in SBF are observed for the MMBG-P123 specimen, although neither of these values change any more after 48 h. This discrepancy apparently comes from the difference in both the pore structure and surface area. MMBG-F127 has a 3D cubic pore structure and a larger surface area and pore volume than MMBG-P123 with its 2D-hexagonal pore structure, both of which enable the former to exhibit a higher diffusion transportation mechanism than the latter, thereby allowing it to show superior bioactive behavior.[6,10] In the case of the NoTri-BG specimen, both the Ca^{2+} levels and pH value slowly increases during the first 48 h, but the increase in the Ca^{2+} level is clearly lower than that of both MMBG-F127 and MMBG-P123. The Ca^{2+} concentration and pH value for the NoTri-BG specimen decrease until 72 h and do not change thereafter. These results indicate that the BG scaffolds, which have a hierarchically mesoporous–macroporous structure may have superior bone-forming bioactivities compared to the general BG scaffolds, consisting of only macropores. Even though NoCaP-MMBG-F127 has the same hierarchical pore structure as MMBG-F127 and that according to Vallet-Regí et al. mesoporous silica also exhibit bioactivity, and there are no changes in the Ca^{2+} level or pH during the tested periods. That is, NoCaP-MMBG-F127 has significantly lower bioactivity than the MMBGs. The chemical compositions of the scaffolds and architectures of the pores are closely related to get capable bioactivity.

The bone-forming activity of the MMBG-F127 (and that of the NoTri-BG for comparison) *in vitro* was tested in SBF to monitor the formation of apatite on the surface of the MMBG over time as shown in Figure 5. Before soaking in SBF solution, both the NoTri-BG and MMBG-F127 showed a smooth and homogeneous surface [Figure 5(a,e)]. The FE-SEM image reveals that the surface of the MMBG undergoes important changes when it reacts with the SBF. It is surprising to note that the surface of the MMBG was fully covered with newly formed apatitelike nanoparticles after soaking for only 1 h [Figure 5(b)], while the NoTri-BG still shows a relatively smooth surface [Figure 5(f)]. The FE-SEM and TEM examinations revealed that the morphology of these nanoparticles consists of platelike shapes about 100 nm in diameter. During the initial 24 h, the covered apatite nanoparticle layer on the surface of the MMBG gradually became thicker and changed to a rodlike morphology, which is similar to the morphology of apatite in human bones [Figure 5(b–d)]. In contrast, there was only a partial apatite precipitation on the surface of the NoTri-BG after soaking it for 24 h [Figure 5(f–h)]. These results indicate that the MMBG had much better ability to induce apatite formation than the NoTri-BG because of the large surface area provided by mesopore as well as macropore. The biomimetic apatite formation behavior of the hierarchically porous BG, containing mesopore, means that the MMBG synthesized by the current strategy possesses outstanding bone-forming activity *in vitro*.

Biocompatibility of MMBG

The biocompatibilities of the MMBG-F127, MMBG-P123, and NoTri-BG specimens were evaluated *in vitro* by studying the MG63 behavior for three passages, viz. 1-day, 4-day, and 7-day, using the MTT test and FE-SEM observation. Figure 6 shows the representative FE-SEM micro-

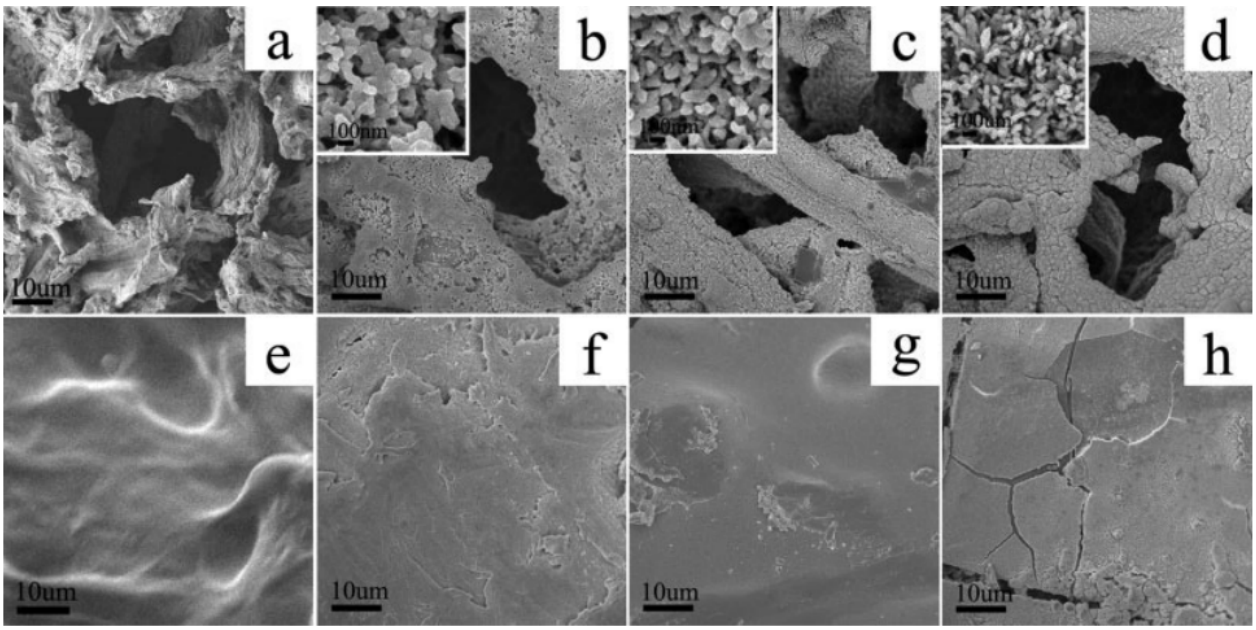

Figure 5. FE-SEM micrographs of (a–d) MMBG-F127 and (e–h) NoTri-BG after immersing them in SBF for (a, e) 0 h, (b, f) 1 h, (c, g) 6 h, and (d, f) 24 h. The insets are the enlarged images of (b–d).

graphs of the attachment of the cells onto the MMBG-F127 specimens before [Figure 6(a)] and after 1 and 7 days [Figure 6(b,c)] of cell culture. From the micrographs, it can be seen that after 1 day of culture, the MG63 cells adhere well onto the MMBG-F127 specimen through the walls of the macropores (the parts indicated by arrows), while no significant cell adhesion is observed for NoTri-BG (data not shown here). These cell behaviors continued with good proliferation and migration onto the MMBG-F127 specimen after 7 days of cell culture. The MMBG-F127 specimen appeared to have no negative effect on the cell morphology, viability, and proliferation at this stage.

The MTT test results also bear out the favorable cell behavior for MMBG-F127, as shown in Figure 7. After 1 day of cell culture, the cell numbers seeded on both MMBG-F127 and MMBG-P123 are significantly larger than that on NoTri-BG. That is, the MMBG-F127 induces better early cell adhesion than the NoTri-BG. No significant statistical difference in the cell numbers between the specimens examined after 1 and 4 days of culture was observed for MMBG-F127, but the cell number increased manifestly after 7 days of culture. A similar ascendant tendency of the cell population was confirmed for MMBG-P123, while the cell numbers seeded on NoTri-BG do not show any meaningful increase in the same period. These results demonstrate that the BGs with both homogeneous mesopores and macropores allow more favorable cell behavior than those without these pore structures. According to the results of this study, we come to the conclusion at this stage that MMBGs have no negative effect on the attachment and proliferation of cells and that they are *in vitro* biocompatible.

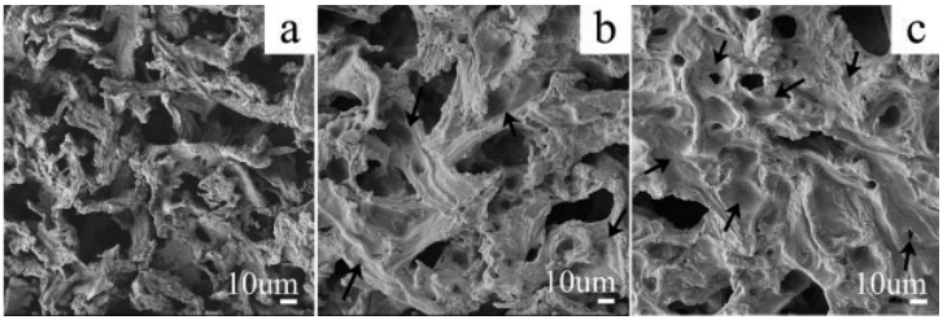

Figure 6. FE-SEM micrographs of MG-63 osteoblastlike cells attached onto the MMBG-F127 scaffolds (a) before and (b) after 1 day, and (c) at 7 days cell culture.

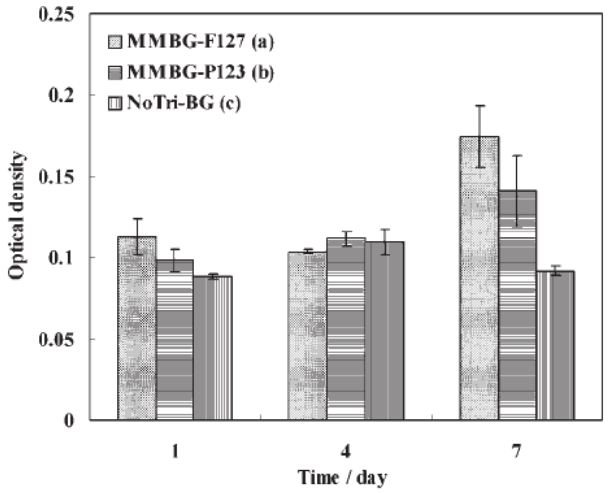

Figure 7. MTT assay for proliferation of MG-63 cultured at various incubation periods onto (a) MMBG-F127, (b) MMBG-P123, and (c) NoTri-BG. Error bars represent means ± SD for $n = 5$.

CONCLUSION

Highly ordered hierarchically mesoporous–macroporous bioactive glasses with a well-interconnected 2D/3D pore structure were synthesized using a multipolymer templating method. The control of both the mesopore structure and the homogeneous distribution of the macropores were successfully achieved. The superior bone-forming bioactivity of the MMBG *in vitro* was also confirmed. The combination of two 2D/3D pore structures with different size ranges, their good molding capabilities as well as compressive strength, their superior *in vitro* bioactivity, and their favorable biocompatibility make the MMBGs promising for use as novel scaffolds for tissue regeneration with controlled drug delivery functionalities. We hope that this simple, reproducible synthetic method can be adapted for the preparation of various hierarchical porous materials, having the potential to be used in applications involving biomedical devices, sensors, filters, catalysis, and optics. More detailed studies of their *in vitro* and *in vivo* properties are currently in progress.

REFERENCES

1. Stein A. Advances in microporous and mesoporous solids - highlights of recent progress. Adv Mater 2003;15:763–775.
2. Hartmann M. Ordered mesoporous materials for bioadsorption and biocatalysis. Chem Mater 2005;17:4577–4593.
3. Vallet-Regí M. Ordered mesoporous materials in the context of drug delivery systems and bone tissue engineering. Chem Eur J 2006;12:5934–5943.
4. Vallet-Regí M, Ruiz-González L, Isabel-Barba I, González-Calbet JM. Revisiting silica based ordered mesoporous materials—Medical applications. J Mater Chem 2006;16:26–31.
5. Isabel-Barba I, Ruiz-González L, Doadrio JC, González-Calbet JM, Vallet-Regí M. Tissue regeneration—A new property of mesoporous materials. Solid State Sci 2005;7:983–989.
6. López-Noriega A, Arcos D, Isabel-Barba I, Sakamoto Y, Terasaki O, Vallet-Regí M. Ordered mesoporous bioactive glasses for bone tissue regeneration. Chem Mater 2006;18: 3137–3144.
7. Yan X, Yu C, Zhou X, Tang J, Zhao D. Highly ordered mesoporous bioactive glasses with superior in vitro bone-forming bioactivities. Angew Chem Int Ed 2004;43:5980–5984.
8. Yan SS, Deng HX, Huang XH, Lu GQ, Qiao SZ, Zhao DY, Yu CZ. Mesoporous bioactive glasses—Synthesis and structural characterization. J Non-Cryst Solid 2005;351:3209–3217.
9. Yan X, Huang X, Yu C, Deng H, Wang Y, Zhang Z, Qiao S, Lu G, Zhao D. The in-vitro bioactivity of mesoporous bioactive glasses. Biomaterials 2006;27:3396–3403.
10. Yun HS, Kim SE, Hyeon YT. Highly ordered mesoporous bioactive glasses with *Im3m* symmetry. Mater Lett 2007: 10.1016/j.matlet.2007.02.075
11. Xia W, Chang J. Well-ordered mesoporous bioactive glasses (MBG)—A promising bioactive drug delivery system. J Control Release 2006;110:522–530.
12. Shi Q, Wang J, Zhang J, Fan J, Stucky GD. Rapid-setting, mesoporous, bioactive glass cements that induce accelerated in vitro apatite formation. Adv Mater 2006;18:1038–1042.
13. Ostomel TA, Shi Q, Tsung CK, Liang H, Stucky GD. Spherical bioactive glass with enhanced rates of hydroxyapatite deposition and hemostatic activity. Small 2006;2:1261–1265.
14. Hollister SJ. Porous scaffold design for tissue engineering. Nat Mater 2005;4:518–524.
15. Koegler WS, Griffith LG. Osteoblast response to PLGA tissue engineering scaffolds with PEO modified surface chemistries and demonstration of patterned cell response. Biomaterials 2004;24:2819–2830.
16. Stevens MM, George JH. Exploring and engineering the cell surface interface. Science 2005;310:1135–1138.
17. Huerta L, Haskouri JE, Vie D, Comes M, Latorre J, Guillem C, Marcos MD, Martínez-Mañez R, Beltrán A, Beltrán D, Amorós P. Nanosized mesoporpous silica coatings on ceramic foams—New hierarchical rigid monoliths. Chem Mater 2007; 19:1082–1088.
18. Yuan ZY, Ren TZ, Azioune A, Pireaus JJ, Su BL. Self-assembly of hierarchically mesoporous–macroporous posphated nanocrystalline aluminum (oxyhydr)oxide materials. Chem Mater 2006;18:1753–1767.
19. Yun HS, Kim SE. Hyun YT. Design and preparation of bioactive glasses with hierarchical pore networks. Chem Commun 2007;(21):2139–2141. DOI: 10.1039/b702103h.
20. Taguchi T, Muraoka Y, Matsuyada H, Kishida A, Akashi M. Apatite coating on hydrophilic polymer-grafted poly(ethylene) films using an alternate soaking process. Biomaterials 2001; 22:53–58.
21. Kokubo T, Takadama H. How useful in SBF in predicting in vivo bone bioactivity? Biomaterials 2007;27:2907–2915.
22. Kundu PP, Kundu M. Effect of salts and surfactant and their doses on the gelation of extremely dilute solutions of methyl cellulose. Polymer 2001;42:2015–2020.
23. Hench LL, Splinter RJ, Allen WC, Greenlee TK. Bonding mechanisms at the interface of ceramics prosthetic materials. J Biomed Mater Res 1972;2:117–141.
24. Hench LL. Bioceramics. J Am Ceram Soc 1998;81:1705–1728.
25. Vallet-Regí M, Ragel CV, Salinas AJ. Glasses with medical applications. Eur J Inorg Chem 2003;(6):1029–1042.
26. Verrier S, Blaker JJ, Maquet V, Hench LL, Boccaccini AR. PDLLA/Bioglass® composites for soft-tissue and hard-tissue engineering: An in vitro cell biology assessment. Biomaterials 2004;25;3013–3021.